Journal of Geodynamics 49 (2010) 141–150

Contents lists available at ScienceDirect

Journal of Geodynamics

journal homepage: http://www.elsevier.com/locate/jog

Kinematics of the eastern part of the North Anatolian Fault Zone

Haluk Ozener[a,*], Esen Arpat[b], Semih Ergintav[c], Asli Dogru[a], Rahsan Cakmak[c], Bulent Turgut[a], Ugur Dogan[d]

[a] Bogazici University, Kandilli Observatory and Earthquake Research Institute, Geodesy Department, Cengelkoy, 34680 Istanbul, Turkey
[b] Bogazici University, Kandilli Observatory and Earthquake Research Institute, Geophysics Department, Cengelkoy, 34680 Istanbul, Turkey
[c] TUBITAK, Marmara Research Center, Earth and Marine Sciences Institute, Gebze, 41470 Kocaeli,, Turkey
[d] Yildiz Technical University, Department of Geodesy and Photogrammetry Engineering, Division of Geodesy, Esenler, 34210 Istanbul, Turkey

ARTICLE INFO

Article history:
Received 27 January 2009
Received in revised form 6 January 2010
Accepted 6 January 2010

Keywords:
North Anatolian Fault Zone
GPS
Kinematics
Velocity field
Strain

ABSTRACT

The North Anatolian Fault Zone (NAFZ), which marks the boundary between Anatolia and the Eurasian plate, is one of the world's most seismically active structures. Although the eastern part of NAFZ has high seismic hazard, there is a lack of geodetic information about the present tectonics of this region. Even though many scientists would like to study this area, geographical and logistical problems make performing scientific research difficult. In order to investigate contemporary neotectonic deformation on the eastern NAFZ and in its neighborhood, a relatively dense Global Positioning System (GPS) monitoring network was established in 2003. Geodetic observations were performed in three GPS campaigns in an area of 350 km × 200 km with 12-month intervals. In addition, 14 new GPS stations were measured far from the deforming area. Since this region includes the intersection of the NAFZ and the East Anatolian Fault Zone (EAFZ), deformation is complex and estimating seismic hazard is difficult. One important segment is the Yedisu segment and it has not broken since the 1784 earthquake. After the 1992 Erzincan and 2003 Pulumur earthquakes, the Coulomb stress loading on the Yedisu segment of the NAFZ has increased significantly, emphasizing the need to monitor this region. We computed the horizontal velocity field with respect to Eurasia and strain rates field as well. GPS-derived velocities relative to Eurasia are in the range of 16–24 mm/year, which are consistent with the regional tectonics. The principal strain rates were derived from the velocity field. Results show that strain is accumulating between the NAFZ and EAFZ along small secondary fault branches such as the Ovacik Fault (OF).

1. Introduction and regional tectonic setting

The North Anatolian Fault Zone (NAFZ) of Turkey is situated at a point where two of the Earth's tectonic plates meet, the Eurasian and Anatolian plates. The 1200 km long NAFZ runs along the northern part of Turkey, from Karliova in the east to the Gulf of Saros in the west and connects the East Anatolian compressional regime to the Aegean extensional regime. So eastern Turkey, the study area where the NAFZ and EAFZ meet, comprises a complicated combination of active plate boundaries (Fig. 1).

Sengor et al. (1985) and Dewey et al. (1986) hypothesized that, due to the northward movement of the Arabian plate relative to Eurasia, the Erzincan–Karliova region is squeezed, crushed, and expelled westward along the NAFZ and EAFZ. As a result of this plate convergence, right-lateral strike-slip faulting along the NAFZ (Sengor, 1979; Dewey and Sengor, 1979; McClusky et al., 2000) and left-lateral strike-slip faulting along the EAFZ (McKenzie, 1972; Jackson and McKenzie, 1988) in eastern Turkey accommodates the westward motion of Anatolia relative to Eurasia.

Several geodynamic models have been proposed to explain the tectonics of the study area, where these two major fault systems join together. Reilinger et al. (2006) find that the principal boundary between the westward moving Anatolian plate and Arabia is currently characterized by left-lateral strike-slip. In this paper, we provide geodetic data from spatially and temporally dense GPS campaigns giving a velocity field representing the active deformation rate in the area and which will serve as a basis for further research.

The Yedisu segment of the NAFZ in the study region was identified as a seismic gap (Barka et al., 1987) and it has not broken since the 1784 earthquake (Ambraseys, 1975). Since geodetic information on the present tectonics of this region is not known very well, it is an ideal one to carry out geodetic crustal deformation investigations. Historic records (Ambraseys, 1970, 1971) reveal

* Corresponding author. Tel.: +90 216 516 3264; fax: +90 216 332 0241.
E-mail addresses: ozener@boun.edu.tr (H. Ozener), esenarpat@gmail.com (E. Arpat), Semih.Ergintav@mam.gov.tr (S. Ergintav), asli.dogru@boun.edu.tr (A. Dogru), Rahsan.Cakmak@mam.gov.tr (R. Cakmak), turgut@boun.edu.tr (B. Turgut), dogan@yildiz.edu.tr (U. Dogan).

0264-3707/$ – see front matter © 2010 Elsevier Ltd. All rights reserved.
doi:10.1016/j.jog.2010.01.003

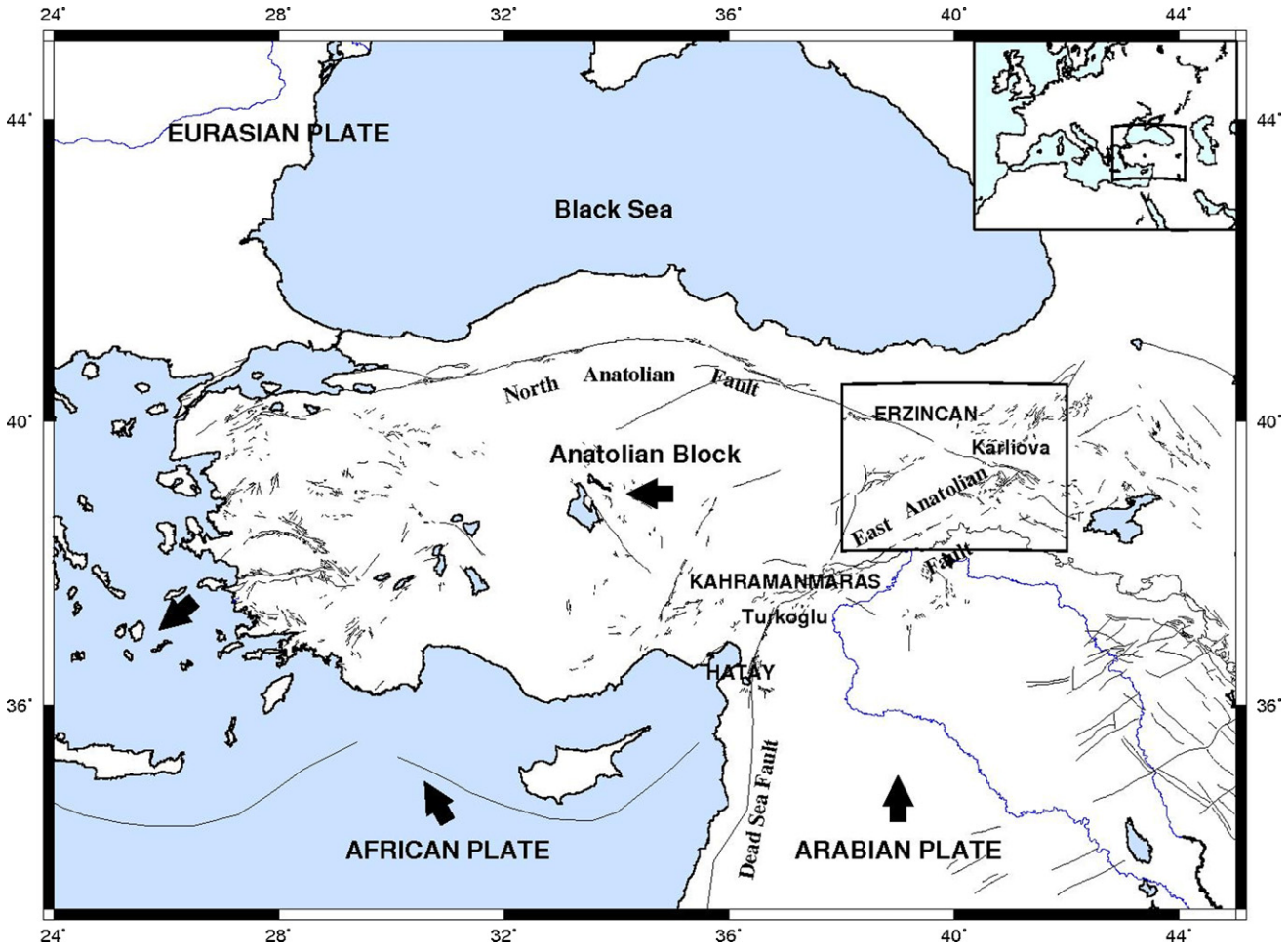

Fig. 1. Tectonic setting of Turkey. Bold arrows show direction of plate motion. The boxed area is the area shown in subsequent figures.

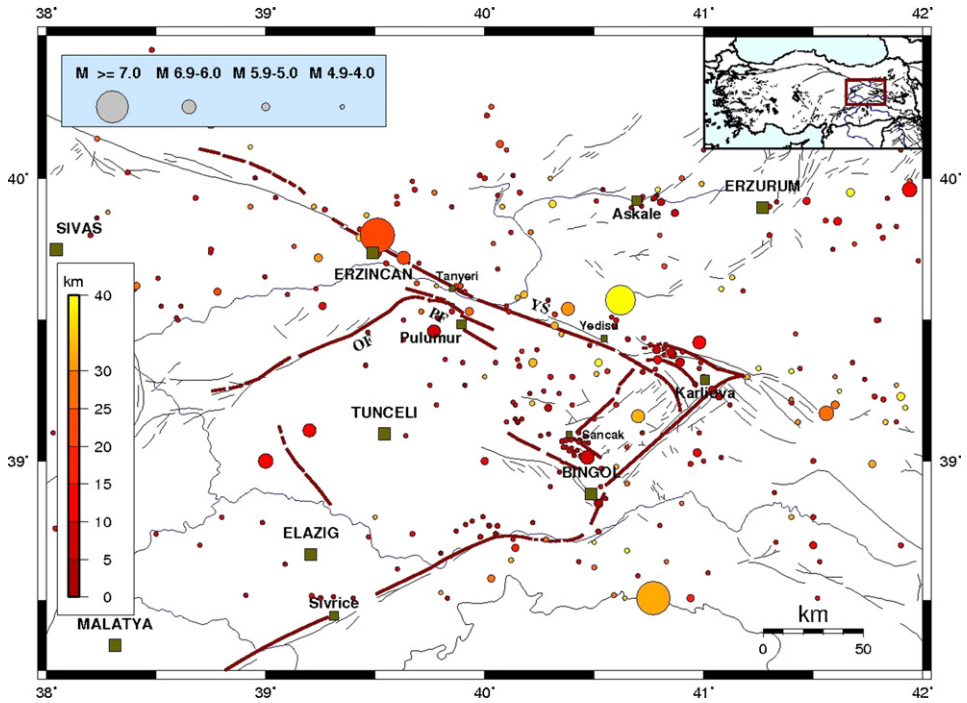

Fig. 2. Regional seismicity since 1900 with known regional faults, bold-red lines indicate the faults surveyed by this project (OF: Ovacik Fault, PF: Pulumur Fault, YS: Yedisu Segment). Colors of the earthquakes represents depth while size represents magnitude (data provided by National Earthquake Monitoring Center of KOERI). (For interpretation of the references to color in this figure legend, the reader is referred to the web version of the article)

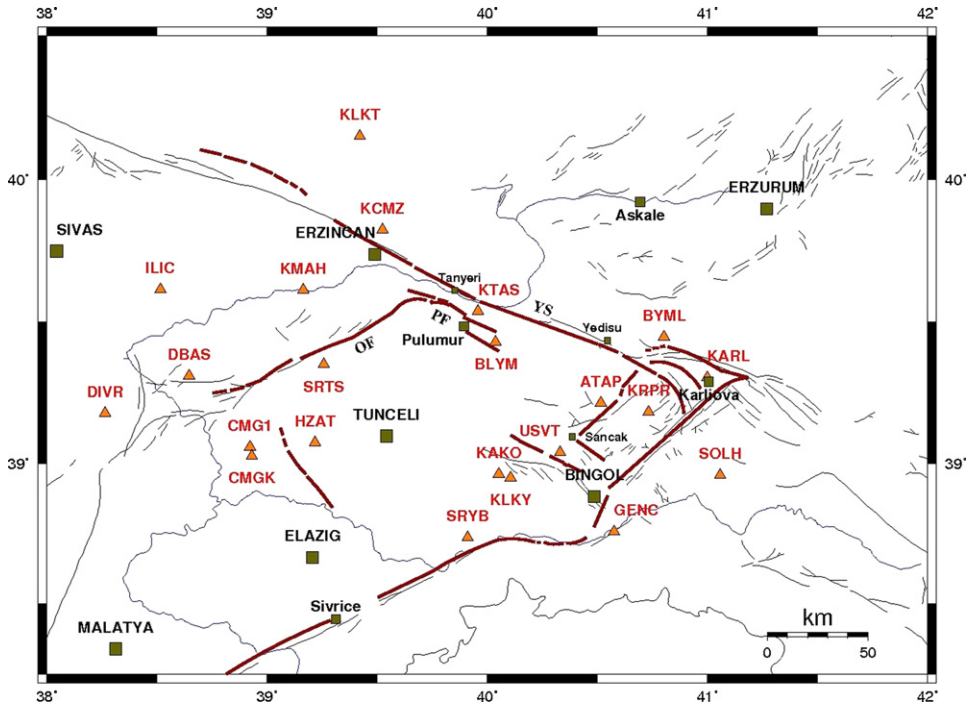

Fig. 3. GPS points used in the present study and active faults (black lines show known regional faults and bold-red lines indicate the faults surveyed by this study). (For interpretation of the references to color in this figure legend, the reader is referred to the web version of the article)

that the EAFZ exhibits occasional large seismic activity (Arpat and Saroglu, 1975). Since the beginning of the 19th century, large earthquakes have been well recorded, providing precise information on their locations and magnitudes, and these events verify the fault lines mapped in that area (Ambraseys, 1989; Saroglu et al., 1992; Ambraseys and Melville, 1995; Ambraseys and Jackson, 1998; Nalbant et al., 2002, 2005) (Fig. 2).

Monitoring tectonic movements in this region is a most challenging activity and a dedicated geodetic network for geodynamic purposes was constructed in the region (Fig. 3). GPS stations were built into bedrock using high quality geodetic monuments. 10-h/day observations were performed at each station in the fall season for 3 years. Additionally, other available GPS sites, having a longer data span, have been included in the present analysis. Observation spans of GPS sites used in this study are summarised in Table 1.

2. Data processing and analysis

The processing of the GPS data was performed with the GAMIT (King and Bock, 2004)/GLOBK (Herring, 2004) software package. Each campaign was processed using the International Terrestrial Reference Frame ITRF2005. Precise final orbits by the International GNSS Service (IGS) were obtained in SP3 (Standard Product 3) format from SOPAC (Scripps Orbit and Permanent Array Center). Earth Rotation Parameters (ERP) came from USNO_bull_b (United States Naval Observatory_bulletin_b). The 9-parameter Berne model was used for the effects of radiation and the pressure. The IERS 2003 model (McCarthy and Petit, 2004) and FES2004 (Letellier, 2004) was used for the solid earth tide and the ocean tide loading effects. Zenith Delay unknowns were computed based on the Saastamoinen a priori standard troposphere model with 2-h intervals. Iono-free LC (L3) linear combination of L1 and L2 carrier phases was used

Table 1
GPS observation spans.

Site	Longitude (°)	Latitude (°)	First epoch	Last epoch	Interval (year)	No.
SOLH	41.057	38.959	2003.344	2006.593	3.25	5
KRPR	40.733	39.182	2003.788	2005.711	1.92	3
GENC	40.575	38.758	2003.344	2006.593	3.25	2
ATAP	40.515	39.215	2003.788	2005.711	1.92	3
USVT	40.330	39.039	2003.788	2005.711	1.92	3
KLKY	40.105	38.949	2003.788	2005.711	1.92	3
KAKO	40.052	38.963	2003.344	2006.593	3.25	2
BLYM	40.038	39.430	2003.788	2004.695	0.91	2
KTAS	39.957	39.538	2003.788	2005.711	1.92	3
SRYB	39.910	38.737	2003.344	2008.540	5.20	5
KCMZ	39.524	39.824	2003.788	2005.711	1.92	3
KLKT	39.420	40.151	2006.560	2008.578	2.02	4
SRTS	39.258	39.350	2003.788	2005.711	1.92	3
HZAT	39.217	39.074	2003.788	2005.711	1.92	3
KMAH	39.164	39.613	2003.788	2008.578	4.79	7
CMG1	38.931	39.026	2003.788	2008.540	4.75	5
DBAS	38.645	39.310	2003.788	2005.711	1.92	3
ILIC	40.673	38.987	2003.344	2008.578	5.23	5
DIVR	38.264	39.178	2003.788	2005.711	1.92	3

Table 2
IGS sites used for ITRF2005 realization.

No.	Site	Long. (°)	Lat. (°)	υ_N (mm/yearr)	υ_E (mm/year)	υ_U (mm/year)	Ref. epoch
1	ALGO	281.929	45.956	0.0025	−0.0159	0.0025	2009.7000
2	AUCK	174.834	−36.603	0.0399	0.0047	−0.0018	2009.6918
3	BAHR	50.608	26.209	0.0299	0.0307	−0.0008	2008.5697
4	BRAZ	312.122	−15.947	0.0131	−0.0043	−0.0001	2009.6890
5	BRMU	295.304	32.370	0.0088	−0.0123	−0.0002	2009.6973
6	CAS1	110.520	−66.283	−0.0103	0.0020	0.0003	2009.6973
7	CHAT	183.434	−43.956	0.0335	−0.0400	−0.0008	2009.6973
8	DAV1	77.973	−68.577	−0.0052	−0.0031	−0.0018	2009.6973
9	DRAO	240.375	49.323	−0.0102	−0.0127	0.0004	2009.6973
10	GODE	283.173	39.022	0.0040	−0.0143	−0.0009	2009.6973
11	GRAZ	15.493	47.067	0.0156	0.0215	0.0000	2009.6973
12	GUAM	144.868	13.589	0.0044	−0.0097	0.0004	2009.6945
13	HOB2	147.439	−42.805	0.0556	0.0144	−0.0013	2009.6973
14	HRAO	27.687	−25.890	0.0181	0.0183	0.0001	2009.6973
15	IRKT	104.316	52.219	−0.0065	0.0251	0.0005	2009.6973
16	KERG	70.256	−49.351	−0.0028	0.0056	0.0002	2009.6973
17	KIT3	66.885	39.135	0.0055	0.0278	−0.0031	2009.6973
18	KOSG	5.810	52.178	0.0162	0.0177	0.0000	2009.6973
19	KOUR	307.194	5.252	0.0134	−0.0037	0.0022	2009.6973
20	MAC1	158.936	−54.500	0.0307	−0.0111	−0.0021	2009.6973
21	MAS1	344.367	27.764	0.0174	0.0158	0.0001	2009.6973
22	MATE	16.704	40.649	0.0194	0.0228	0.0017	2009.6973
23	MDO1	255.985	30.681	−0.0053	−0.0120	0.0005	2009.6973
24	NLIB	268.425	41.772	−0.0012	−0.0150	−0.0012	2009.6973
25	NYAL	11.865	78.930	0.0136	0.0102	0.0072	2009.6973
26	ONSA	11.926	57.395	0.0145	0.0169	0.0031	2009.6973
27	PERT	115.885	−31.802	0.0599	0.0411	−0.0034	2009.6973
28	PIE1	251.881	34.302	−0.0068	−0.0126	0.0011	2009.6973
29	TIDB	148.980	−35.399	0.0558	0.0183	−0.0018	2009.6973
30	TROM	18.938	69.663	0.0152	0.0147	0.0024	2009.3411
31	TSKB	140.087	36.106	−0.0075	−0.0027	0.0004	2009.6973
32	VILL	356.048	40.444	0.0169	0.0189	−0.0007	2009.6973
33	WES2	288.507	42.613	0.0051	−0.0151	−0.0011	2009.6973
34	WTZR	12.879	49.144	0.0155	0.0200	−0.0004	2009.6973
35	YELL	245.519	62.481	−0.0109	−0.0171	0.0055	2009.6973

(Ergintav et al., 2009). The model, which depended on the height, was preferred for the phase centres of the antennas. Losely constrained daily solutions obtained from GAMIT were included in the ITRF2005 reference frame by a 7 parameters (3 offset–3 rotation–1 scale) transformation with 35 global IGS stations. The selected IGS sites for reference frame definition and their velocities in a local system are given in Table 2.

Station velocities were obtained from trend analysis by time series that were formed by daily precise coordinates combined with Kalman analysis (Ozener et al., 2005). Velocities in the region determined by GPS campaigns are summarised in Table 3 and shown in Fig. 4. Outliers larger than 2σ were discarded. We found unrealistic velocity values in the KARL and BYML stations by analyzing the results of GPS data process. In order to investigate the causes, the major earthquakes that occurred in the region during the project were examined. Data were taken from the Global Centroid Moment Tensor (CMT) catalogue and summarised in Table 4. Fig. 5 shows the focal mechanism solutions of these earthquakes. It is seen that the region was affected by a series of earthquakes during the study and that some sites display the co-seismic

Table 3
Horizontal GPS velocities in the Eurasia-fixed reference frame and 1-sigma uncertainties (plotted with 95% confidence ellipses in Fig. 4). RHO is the correlation coefficient between the E (east) and N (north) uncertainties.

Site	Lon. (°)	Lat. (°)	E_{vel} (mm/year)	N_{vel} (mm/year)	E_{sig} (mm/year)	N_{sig} (mm/year)	RHO
SOLH	41.057	38.959	−9.32	14.57	0.66	0.64	−0.075
KRPR	40.733	39.182	−15.71	4.73	1.67	2.13	−0.062
GENC	40.575	38.758	−4.95	17.14	0.71	0.69	−0.131
ATAP	40.515	39.215	−18.00	5.35	1.62	2.13	−0.076
USVT	40.330	39.039	−20.20	7.90	1.96	2.58	−0.101
KLKY	40.105	38.949	−17.33	6.23	0.62	0.67	−0.043
KAKO	40.052	38.963	−17.33	6.23	0.62	0.67	−0.043
BLYM	40.038	39.430	−13.31	8.51	3.25	4.24	−0.053
KTAS	39.957	39.538	−12.76	2.89	1.52	1.88	−0.075
SRYB	39.910	38.737	−18.76	11.13	0.61	0.59	−0.072
KCMZ	39.524	39.824	−7.36	−1.39	1.18	1.47	−0.053
KLKT	39.420	40.151	−4.97	2.40	0.35	0.38	−0.034
SRTS	39.258	39.350	−19.25	4.12	1.28	1.59	−0.051
HZAT	39.217	39.074	−20.63	12.10	1.50	1.86	−0.069
KMAH	39.164	39.613	−14.80	8.73	0.40	0.51	−0.100
CMGK	38.931	39.026	−19.06	12.58	0.83	0.98	−0.089
CMG1	38.922	39.059	−19.06	12.58	0.83	0.98	−0.089
DBAS	38.645	39.310	−21.90	9.77	1.37	1.67	−0.085
ILIC	38.515	39.614	−20.04	10.79	0.41	0.49	−0.113
DIVR	38.264	39.178	−17.01	12.90	1.34	1.59	−0.104

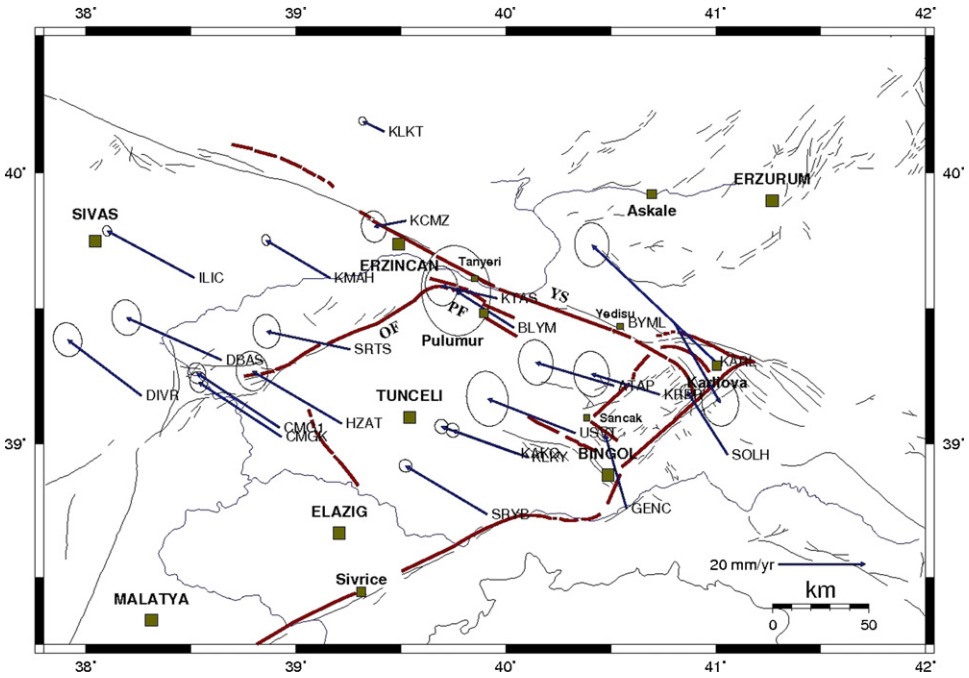

Fig. 4. Horizontal velocity field of the region in the Eurasia-fixed reference frame (ellipses are at 95% confidence level).

signature of the earthquakes. Fig. 6 shows two stations' GPS time series between the years of 2003 and 2007. They show significant co-seismic motion related to the 2005–2006 earthquake sequences.

Stations have northwest directed displacements relative to Eurasia, consistent with the right-lateral NAFZ. Table 5 and Fig. 7 show the estimated velocities relative to a reference point (ILIC) located outside of the main deforming area in order to highlight the local velocities in the eastern part of Anatolia.

2.1. Strain pattern in the region

In order to estimate a strain rate and velocity model, the method developed by Haines and Holt (1993) was employed. A comprehensive overview of the methodology can be found in Haines et al. (1998). The grid model (Garagon Dogru, 2008; Ozener et al., 2009) is continuous in the longitude and latitude directions and covers Turkey. The Eurasian, African and Arabian plates are rigid areas such that the distance between any two given points remains constant. All other areas are considered to be deforming. The extent of the rigid blocks is based on seismicity (Ambraseys and Finkel, 1995; Global CMT Catalog; KOERI Earthquake Catalog).

According to Haines and Holt (1993), three components of the strain rate tensor determine a rotation vector function, and it describes the horizontal velocity field $u(r)$ expressed as

$$u(\hat{x}) = rW(\hat{x}) \times \hat{x}$$

where r is the radius of the Earth and $\hat{x}$ is the position vector on the Earth's surface. The associated horizontal components of strain rate are given by

$$\varepsilon_{\phi\phi} = \frac{\Theta}{\cos\theta} \cdot \frac{\partial W}{\partial \phi},$$

$$\varepsilon_{\phi\theta} = \frac{1}{2}\left(\Theta \cdot \frac{\partial W}{\partial \theta} - \frac{\Phi}{\cos\theta} \cdot \frac{\partial W}{\partial \phi}\right),$$

$$\varepsilon_{\theta\theta} = -\Phi . \frac{\partial W}{\partial \theta}$$

with ϕ and θ being longitude and latitude, respectively, and

$$\Phi = (-\sin\phi,\ \cos\phi, 0)$$

$$\Theta = (-\sin\theta\cos\phi,\ -\sin\theta\sin\phi,\ \cos\theta)$$

being the unit vectors in the east and north directions. Any region, where $W(r)$ is constant, is rigid. A Bessel form of a bi-cubic spline interpolation is used to make strain rates continuous at the nodes of the grid. These values are obtained from the least-squares inversion between the observed and predicted values of strain rate and velocity.

Fig. 8 displays a present-day deformation field obtained from the GPS velocities. In order to minimize the effects of the large-

Table 4
Fault plane parameters of large earthquakes occurring during the study.

No.	Location	Date d/m/y	Time h/m/s	Lat. N (°)	Lon. E (°)	Depth (km)	Seismic M. Mo	Magnitude M_w	Fault plane parameters strike/dip/slip	
1	Askale (Erzurum)	25.03 2004	19:30:54.6	40.05	40.70	16.4	3.26E+24	5.6	280/80/−173	188/83/−10
2	Askale (Erzurum)	28.03.2004	03:51:16.3	40.07	40.74	18.9	2.80E+24	5.6	179/79/2	89/88/169
3	Sivrice (Elazig)	11.08.2004	15:48:30.1	38.50	39.09	14.3	3.60E+24	5.6	245/83/−4	335/86/−173
4	Karliova (Bingol)	12.03.2005	07:36:15.0	39.42	40.79	16.1	3.52E+24	5.6	191/70/−15	286/76/−159
5	Karliova (Bingol)	14.03.2005	01:56:01.6	39.44	40.77	12.0	6.08E+24	5.8	287/75/−165	194/76/−15
6	Karliova (Bingol)	23.03.2005	21:44:56.4	39.42	40.71	15.1	3.12E+24	5.6	188/77/13	281/77/−167
7	Karliova (Bingol)	06.06.2005	07:41:33.9	39.44	40.87	15.4	3.66E+24	5.6	293/71/−167	199/78/−19
8	Karliova (Bingol)	10.12.2005	00:09:54.5	39.48	40.75	20.3	1.69E+23	5.4	277/76/−177	186/87/−14
9	Karliova (Bingol)	02.07.2006	19:39:44.2	39.49	40.78	15.0	3.58E+23	5.0	290/63/−163	192/75/−28

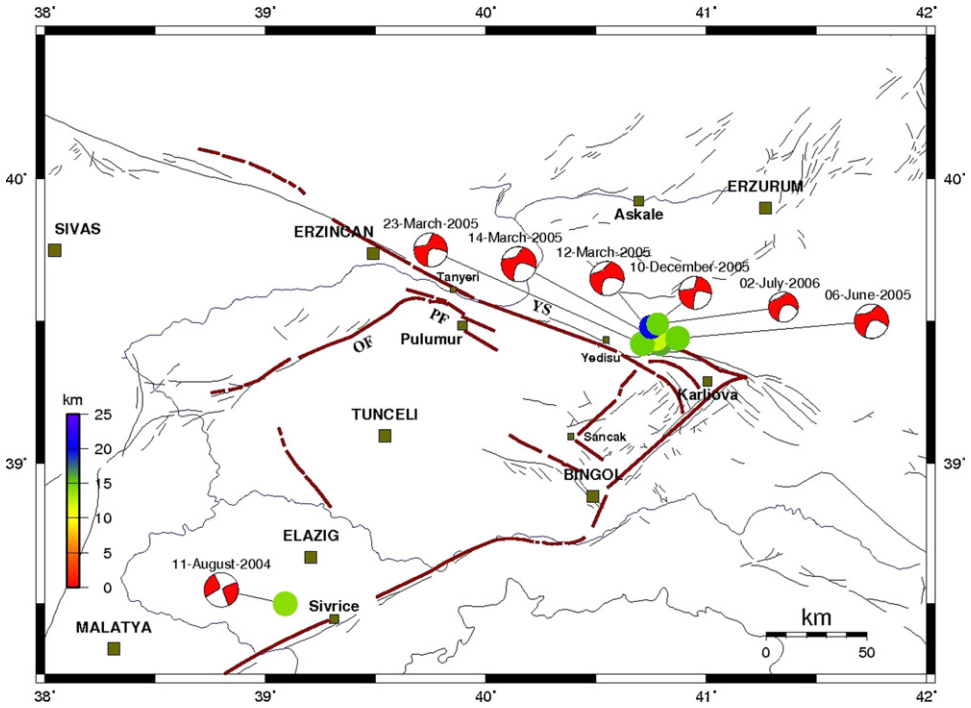

Fig. 5. Focal mechanism solutions of earthquakes with $M_w > 4.0$ during the period of this study (Colors represent focal depths, as given by the scale in the bottom left corner). (For interpretation of the references to color in this figure legend, the reader is referred to the web version of the article)

scale strain rates, the velocities relative to the ILIC reference point were used. The results are given in Table 6. As can be seen from the figure, stations KRPR, USVT, KAKO, KLKY show significant extension.

3. Results and discussion

The North Anatolian Fault Zone (NAFZ), intersects the left-lateral strike-slip East Anatolian Fault Zone (EAFZ) about 10 km

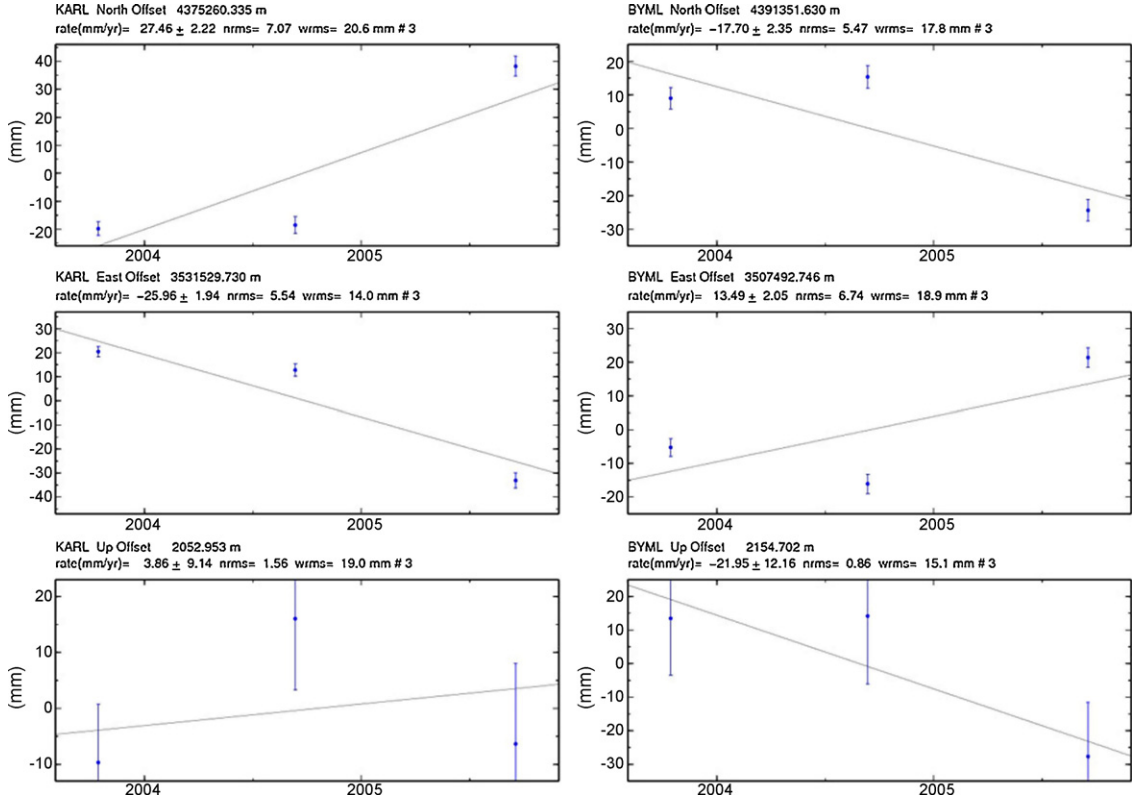

Fig. 6. GPS time series of KARL and BYML stations between 2003 and 2006, which show the significant co-seismic motion of 2005–2006 earthquake sequences.

Table 5
Horizontal GPS velocities relative to ILIC.

Site	Lon. (°)	Lat. (°)	E_{vel} (mm/year)	N_{vel} (mm/year)	E_{sig} (mm/year)	N_{sig} (mm/year)	RHO
SOLH	41.057	38.959	10.72	3.78	0.77	0.80	−0.087
KRPR	40.733	39.182	4.33	−6.06	1.71	2.18	−0.065
GENC	40.575	38.758	15.09	6.35	0.82	0.85	−0.126
ATAP	40.515	39.215	2.04	−5.44	1.67	2.18	−0.078
USVT	40.330	39.039	−0.16	−2.89	2.00	2.63	−0.102
KLKY	40.105	38.949	2.71	−4.56	0.74	0.83	−0.066
KAKO	40.052	38.963	2.71	−4.56	0.74	0.83	−0.066
BLYM	40.038	39.430	6.73	−2.28	3.27	4.27	−0.054
KTAS	39.957	39.538	7.28	−7.90	1.57	1.94	−0.078
SRYB	39.910	38.737	1.28	0.34	0.73	0.76	−0.086
KCMZ	39.524	39.824	12.68	12.18	1.24	1.55	−0.059
KLKT	39.420	40.151	15.07	−8.39	0.54	0.62	−0.081
SRTS	39.258	39.350	0.79	−6.67	1.34	1.66	−0.056
HZAT	39.217	39.074	−0.59	1.32	1.55	1.92	−0.072
KMAH	39.164	39.613	5.24	−2.06	0.56	0.69	−0.107
CMGK	38.931	39.026	0.98	1.79	0.92	1.09	−0.094
CMG1	38.922	39.059	0.98	1.79	0.92	1.09	−0.094
DBAS	38.645	39.310	−1.86	−1.01	1.43	1.74	−0.087
DIVR	38.264	39.178	3.03	2.11	1.40	1.67	−0.105

east-northeast of the Karliova district (Arpat and Saroglu, 1972). The EAFZ is one of the main active fault systems in Turkey. It runs in a southwesterly direction from Karliova in the northeast to the province of Kahramanmaras in the southwest where, in the Turkoglu region, its orientation changes to a more southerly direction continuing to the province of Hatay and onto the Dead Sea Fault (Fig. 1). The EAFZ is about 600 km in length and the width of the fault zone varies between 2 and 30 km. Its slip rate is about 10 mm/year. There have been no destructive earthquakes on the EAFZ for 140 years, with the exception of the 1971 Bingol earthquake.

The NE-SW trending Ovacik Fault OF (Arpat and Saroglu, 1972) intersects the NAFZ southeast of the pull-apart Erzincan basin (Kaypak and Eyidogan, 2002). It is a left-lateral strike-slip fault runs from east of the Erzincan basin to southwest of Ovacik, then intersects with the Malatya fault. It is about 160 km in length (Demirtas and Yilmaz, 2006). The fault plane solution of the January 27, 2003 Pulumur earthquake, that took place at the beginning of this project is 60° strike, 71° dip, −13° slip/rake. The focal depth is 10 km and the seismic moment of the earthquake is 1.323×10^{18} Nm. Although predominantly left-lateral strike-slip, the earthquake displayed a normal fault component as well. This earthquake ($M = 6.1$) is located at the end of the OF; no destructive earthquake has yet occurred on the OF (Tan and Taymaz, 2003).

The 2005 Bingol earthquakes (Table 4) and aftershocks also occurred in the study area. This Bingol earthquake sequence affected the GPS results with two sites (KARL and BYML) showing their total co-seismic signature. The study region is not controlled very well seismologically and geodetically and these GPS data supply valuable information about the relation between fault segments and earthquakes, which have larger location errors.

The Yedisu segment of NAFZ is the longest fault in the study area (Fig. 3). This segment has not produced a recorded seismic event in the near past and is considered as a 70-km length seismic gap.

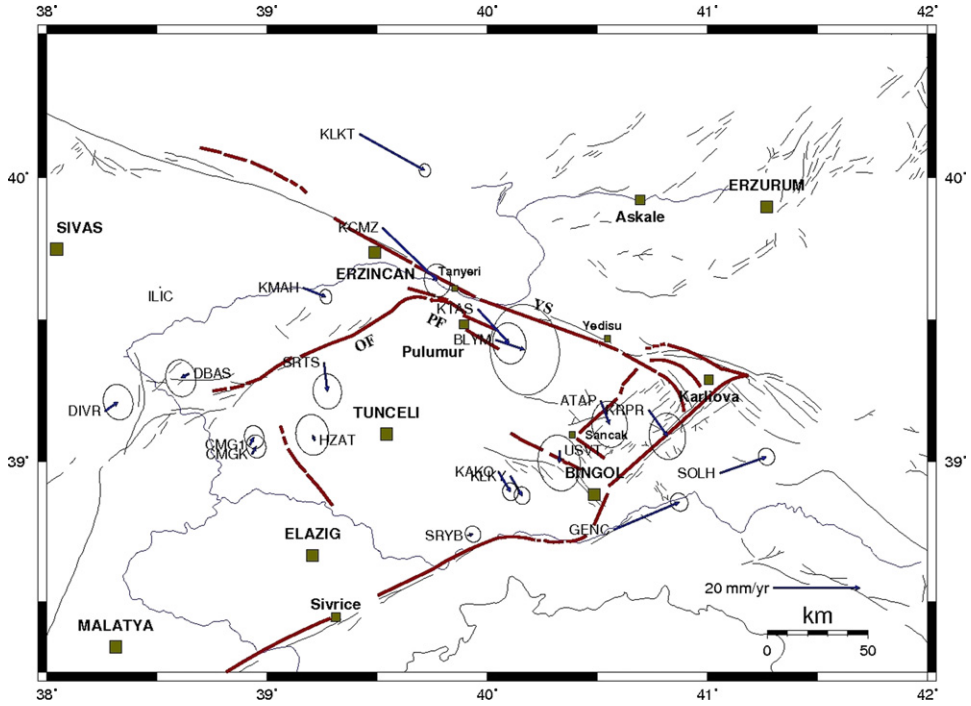

Fig. 7. Horizontal velocity field of the region relative to ILIC (ellipses are at 95% confidence level).

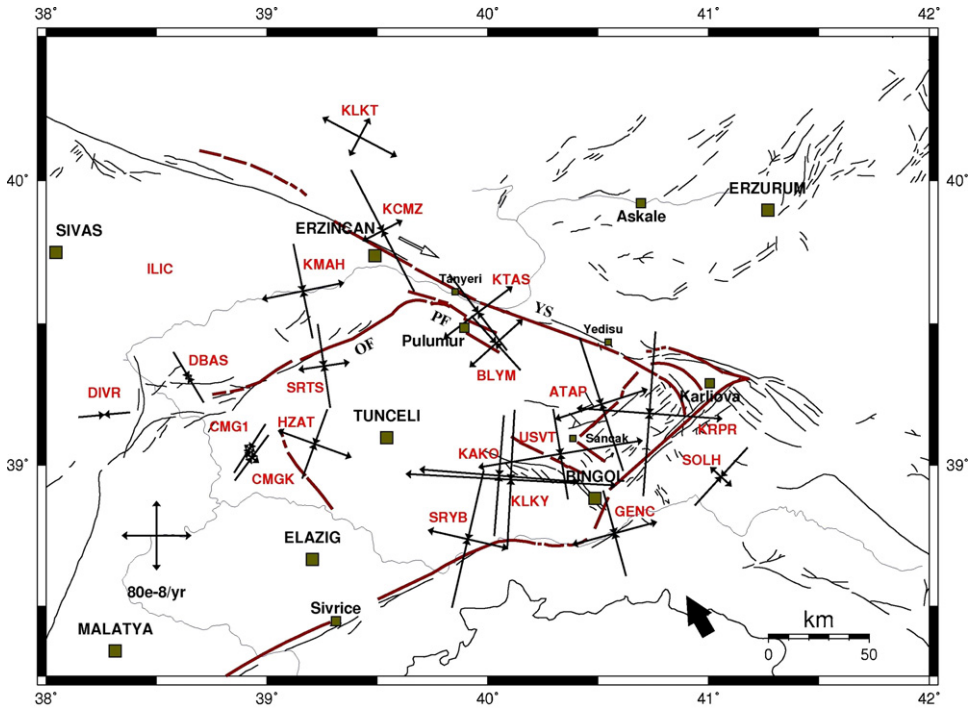

Fig. 8. Principal strain rates (ε_1 and ε_2) for the region from the inversion of GPS velocities relative to ILIC. Inward arrows indicate compression directions and outward arrows indicate extension directions.

The 2003 Bingol and Pulumur earthquakes indicate that cross-fault systems between the NAFZ and EAFZ trigger each other. Therefore, the faults between Bingol–Karliova–Erzincan region, which have not produced an earthquake in the last century, are the faults with the greatest potential to produce earthquakes in the region (Emre et al., 2005). The March 12 and 14, 2005 Karliova earthquakes, with $M_l = 5.7$ ($M_w = 5.8$ by Harward) and $M_l = 5.9$ ($M_w = 5.6$ by Harward), respectively, occurred closely to the west of the intersection of the NAFZ and EAFZ. The focal depths of both are 5 km. The fault plane solutions indicate that they were caused by WNW-ENE aligned faults, in agreement with the orientation of the NAFZ. The Yedisu Fault, where there has not been significant stress relaxation since 1784, has the potential to produce an event with a magnitude between 6.7 and 7 when considering fault length–earthquake magnitude relationships based on previous seismicity. In addition, considering stress transfer to the west along right-lateral strike-slip faults, these recent earthquakes may increase the stress on the Yedisu fault segment (Tuysuz and Erturac, 2005). These discussions are based on simple fault geometries and kinematics. In this study, we emphasize the importance of secondary faults and the slip partitioning between these and the Yedisu segment. This possible slip partitioning may reduce the expected seismic hazard along the Yedisu segment.

It appears that the present morphology of the Karliova region in eastern Anatolia cannot be explained by considering its barely compressional behavior. Considering the NAFZ as a whole, it seems that its motion cannot be caused by the compression of east Anatolia only.

In order to find out the answers to the questions posed in this context, doing an investigation on the region between NAFZ and EAFZ including Karliova was a challenge. Some results obtained from the geodetic observations are listed as follows:

Table 6
Principal strains computed at GPS sites.

Site	Lon. (°)	Lat. (°)	ε_1 (10^{-8} year^{-1})	ε_2 (10^{-8} year^{-1})	Azimuth (°)
SOLH	41.057	38.959	−4.49E+01	1.67E+01	132.30590
KRPR	40.733	39.182	−9.48E+01	8.39E+01	94.21171
GENC	40.575	38.758	−5.10E+01	5.05E+01	74.87037
ATAP	40.515	39.215	−8.05E+01	5.59E+01	72.02650
USVT	40.330	39.039	−5.24E+01	9.56E+01	80.67857
KLKY	40.105	38.949	−8.04E+01	1.21E+02	93.14712
KAKO	40.052	38.963	−6.96E+01	9.17E+01	94.49807
BLYM	40.038	39.430	−4.20E+01	4.12E+01	47.95006
KTAS	39.957	39.538	−5.47E+01	4.95E+01	52.87193
SRYB	39.910	38.737	−8.09E+01	4.71E+01	102.93350
KCMZ	39.524	39.824	−7.86E+01	2.56E+01	62.49331
KLKT	39.420	40.151	2.46E+01	4.84E+01	117.80980
SRTS	39.258	39.350	−4.85E+01	2.96E+01	81.58378
HZAT	39.217	39.074	−4.23E+01	4.47E+01	109.98510
KMAH	39.164	39.613	−5.52E+01	4.83E+01	78.51629
CMGK	38.931	39.026	−3.25E+01	1.00E+01	126.45660
CMG1	38.922	39.059	−3.34E+01	7.08E+00	122.70270
DBAS	38.645	39.310	−3.39E+01	4.45E+00	58.99918
DIVR	38.264	39.178	−2.98E+01	0.85E+00	174.93390

- The velocity difference between the points of SOLH–USVT and ATAP verifies a 9 mm/year velocity difference across the EAFZ.
- The velocity difference between the KLKY–USTV group and the ATAP–KRPR group indicates strain accumulation along the fault running between Bingol and Sancak.
- GENC and SOLH are on the Arabian plate and give an indication for the motion of the Arabian plate in the region.
- Stress patterns in the area covered by CMGK, HZAT, DBAS, and SRTS suggest that strain has been accumulating that may cause left-lateral release. The western segment of the OF has a distinct morphological aspect showing that it is active. This segment alone is 63 km long. Taking into consideration its intraplate nature and low strain rate, it can be deduced that it may generate earthquakes with magnitudes 7.1–7.2 with a rather long recurrence interval.
- East–west compression and north–south extension of KCMZ, KTAS and BLYM is closely related to right-lateral faulting with respect to NAFZ.
- In the area between ATAP, KRPR, USVT, KLKY, KAKO, SRYB, maximum direction of shear rotates from east to west and defines a rotation of that. It is the result of a significant rotation as a slip partioning between different secondary faults.
- KMAH and SRTS show shear but KMAH is bigger than SRTS and this reflects strain accumulation along OF.
- While SOLH shows significant compression, strain at GENC indicate pure shear.
- Compression is dominant in the region covered by DIVR, DBAS and CMGK and OF but cannot extend westward within Anatolia. This gives an important virtual border of the internal deformation zone between Yedisu-EAFZ and OF.
- This internal deformation between Yedisu-EAFZ and OF can be an indication of slip partitioning between secondary fault zones and the Yedisu segment. Accordingly, this process can reduce the strain accumulation along the Yedisu segment and seismic hazard along the Yedisu, which has previously ignored the importance of secondary faults in the region, should be re-interpreted.

4. Conclusions

Although several geodetic studies have been carried out on the NAFZ and EAFZ, this study is the first and only GPS geodynamic research covering the region in terms of its details and its high density of GPS stations. Our results show that strain has been accumulating on the OF and can be large enough to produce large earthquake. On the other hand, internal deformation can reduce stress loading on the Yedisu segment, which can in turn reduce the strain accumulation and hazard scenarios along the Yedisu segment. It is obvious that GPS is the most powerful tool for estimating tectonic loading on the identified active faults. Our aim is to extend the GPS network and continue the study. We conclude and strongly recommend that GPS studies with spatially and temporally dense networks, and preferably with continuously operating reference stations (CORS), should be maintained in order to minimize the hazard in seismically active areas.

Acknowledgements

Authors would like to thank Levent Gulen and Dogan Kalafat for their contribution to the project. Onur Yilmaz and M. Olcay Korkmaz are acknowledged for their support with GPS data collection and monumentation, respectively. We thank project's members and also officials and local people in the region for their help. We would also like to thank Robert Reilinger for his helpful comments that improve the manuscript. We are grateful to Bill Holt and John Haines for their open source Sparse programs. Maps were drawn using GMT 3.4 (Wessel and Smith, 2001). This study was mainly supported by TUBITAK-CAYDAG under Grant No. 103Y043. Additional support was provided by Bogazici University, Kandilli Observatory and Earthquake Research Institute.

References

Ambraseys, N.N., 1970. Some characteristic features of the North Anatolian Fault Zone. Tectonophysics 9, 143–165.
Ambraseys, N.N., 1971. Value of historical records of earthquakes. Nature 232, 375–379.
Ambraseys, N.N., 1975. Studies in historical seismicity and tectonics. Geodynamics Today 7–16, The Royal Soc., London, UK.
Ambraseys, N.N., 1989. Temporary seismic quiescence: SE Turkey. Geophysical Journal 96, 311–331.
Ambraseys, N.N., Finkel, C.F., 1995. The Seismicity of Turkey and Adjacent Areas: A Historical Review, 1500–1800. Eren, Istanbul, Turkey.
Ambraseys, N.N., Melville, C.P., 1995. Historical evidence of faulting in Eastern Anatolia and Northern Syria. Annali Di Geofisica 38, 337.
Ambraseys, N.N., Jackson, J., 1998. Faulting associated with historical and recent earthquakes in the Eastern Mediterranean region. Geophysical Journal International 133, 390–406.
Arpat, E., Saroglu, F., 1972. The East Anatolian Fault system: thoughts on its development. Bulletin of the Mineral Research and Exploration Institute of Turkey 78, 33–39.
Arpat, E., Saroglu, F., 1975. Some significant tectonic events in Turkey. Bulletin of Geology Institution of Turkey 18, 91–101 (in Turkish).
Barka, A.A., Toksoz, M.N., Gulen, L., Kadinsky-Cade, K., 1987. Segmentation, seismicity, and earthquake potential of the eastern part of the North Anatolian Fault Zone. Bulletin of the Earth Sciences Application and Research Center of Hacettepe University 14, 337–352.
Demirtas, R., Yilmaz, R., 2006. Seismotectonics of Turkey. General Directorate of Disaster Affairs, Earthquake Research Agency, http://angora.deprem.gov.tr/rapor.htm (in Turkish).
Dewey, J.F., Sengor, A.M.C., 1979. Aegean and surrounding region: complex multiplate and continuum tectonics in a convergent zone. Geological Society of America Bulletin 90 (1), 84–92.
Dewey, J.F., Hempton, M.R., Kidd, W.S., Saroglu, F., Sengor, A.M.C., 1986. Shortening of continental lithosphere: the neotectonics of eastern Anatolia—a young collision zone. In: Coward, M.P., Ries, A.C. (Eds.), Collision Tectonics, 19. Spec. Publ. Geol. Soc. Lond., pp. 3–36.
Emre, O., Ozalp, S., Yildirim, C., Ozaksoy, V., Dogan, A., 2005. Evaluation of March 12 and 14, 2005 Karliova Earthquakes. General Directorate of Mineral Research and Exploration, Geological Surveys Agency, Earth Dynamics Research and Evaluation Coordinatory, Active Tectonics Research Department, Turkey, http://www.mta.gov.tr/deprem/ (in Turkish).
Ergintav, S., McClusky, S., Hearn, E.H., Reilinger, R.E., Cakmak, R., Herring, T., Ozener, H., Lenk, O., Tari, E., 2009. Seven years of postseismic deformation following the 1999, M = 7.4 and M = 7.2, Izmit-Düzce, Turkey earthquake sequence. Journal of Geophysical Research-Solid Earth 114, B07403, doi:10.1029/2008JB006021.
Garagon Dogru, A., 2008. Integration of data related to earthquakes from a variety of disciplines in a Web-GIS, Ph.D. Thesis, Institute of Science and Technology, Istanbul Technical University, Istanbul, Turkey.
Global CMT Catalog, 2006. Global Centroid Moment Tensor Project, http://www.globalcmt.org.
Haines, A.J., Holt, W.E., 1993. A procedure to obtain the complete horizontal motions within zones of distributed deformation from the inversion of strain rate data. Journal of Geophysical Research 98, 12,057–12,082.
Haines, A.J., Jackson, J.A., Holt, W.E., Agnew, D.C., 1998. Representing Distributed Deformation by Continuous Velocity Fields. Institute of Geological and Nuclear Sciences, Wellington, New Zealand, Science Report, 98/5.
Herring, T.A., 2004. GLOBK Global Kalman Filter VLBI and GPS Analysis Program. Massachusetts Institute of Technology, Cambridge, MA, USA.
Jackson, J., McKenzie, D., 1988. The relationship between plate motions and seismic tremors, and the rates of active deformation in the Mediterranean and Middle East. Royal Astronomical Society Geophysical Journal 93, 45–73.
Kaypak, B., Eyidogan, H., 2002. Determination of upper-crust velocity structure (1-D) of the Erzincan basin and its surroundings. ITU Journal/d Engineering 1 (2), 107–122 (in Turkish).
King, R.W., Bock, Y., 2004. Documentation of the MIT GPS Analysis Software: GAMIT. Massachusetts Institute of Technology, Cambridge, MA.
2008. KOERI Earthquake Catalog. National Earthquake Monitoring Center of Bogazici University, Kandilli Observatory and Earthquake Research Institute, Turkey.
Letellier, T., 2004. Etude des ondes de marée sur les plateux continentaux. Thèse doctorale, Université de Toulouse III, Ecole Doctorale des Sciences de l'Univers, de l'Environnement et de l'Espace, 237 p.
McCarthy, D.D., Petit, G., 2004. IERS Conventions (2003), IERS Technical Note 32. Verlag des Budesamts fur Kartographie und Geodasie, Frankfurt.
McClusky, S., Balassanian, S., Barka, A., Demir, C., Ergintav, S., Georgiev, I., Gurkan, O., Hamburger, M., Hurst, K., Kahle, H., Kastens, K., Kekelidze, G., King, R., Kotzev, V., Lenk, O., Mahmoud, S., Mishin, A., Nadariya, M., Ouzounis, A., Paradissis, D., Peter, Y., Prilepin, M., Reilinger, R., Sanli, I., Seeger, H., Tealeb, A., Toksoz, M.N., Veis, G., 2000. Global Positioning System constraints on plate kinematics and

dynamics in the eastern Mediterranean and Caucasus. Journal of Geophysical Research 105, 5695–5719.
McKenzie, D., 1972. Active tectonics of the Mediterranean region. Geophysical Journal of the Royal Astronomical Society 30 (2), 109–185.
Nalbant, S.S., McCloskey, J., Steacy, S., Barka, A.A., 2002. Stress accumulation and increased seismic risk in eastern Turkey. Earth and Planetary Science Letters 195, 291–298.
Nalbant, S.S., McCloskey, J., Steacy, S., 2005. Lessons on the calculation of static stress loading from the 2003 Bingol, Turkey earthquake. Earth and Planetary Science Letters 235, 632–640.
Ozener, H., Dogru, Garagon, A., Turgut, B., Yilmaz, O., Ergintav, S., Cakmak, R., Sanli, U., Arpat, E., Gulen, L., Gurkan, O., March 28–April 1 2005. Investigation of crustal deformation and block kinematics along the eastern sector of the North Anatolian Fault by GPS technique. In: Proceedings of the 10th Technical and Scientific Map Assembly of Turkey, Ankara, Turkey (in Turkish).
Ozener, H., Dogru, A., Unlutepe, A., 2009. An approach for rapid assessment of seismic hazard in Turkey by continuous GPS data. Sensors 9 (1), 602–615.
Reilinger, R., McClusky, S., Vernant, P., Lawrence, S., Ergintav, S., Cakmak, R., Ozener, H., Kadirov, F., Guliev, I., Stepanyan, R., Nadariya, M., Hahubia, G., Mahmoud, S., Sakr, K., ArRajehi, A., Paradissis, D., Al-Aydrus, A., Prilepin, M., Guseva, T., Evren, E., Dmitrotsa, A., Filikov, S.V., Gomez, F., Al-Ghazzi, R., Karam, G., 2006. GPS constraints on continental deformation in the Africa-Arabia-Eurasia continental collision zone and implications for the dynamics of plate interactions. Journal of Geophysical Research 111, B05411, doi:10.1029/2005jb004051.
Saroglu, F., Emre, O., Kuscu, I., 1992. The East Anatolian Fault Zone of Turkey. Annales Tectonicae supplement to volume VI (special issue), 99–125.
Sengor, A.M.C., 1979. The North Anatolian transform fault: its age, offset and tectonic significance. Journal of the Geological Society 136 (3), 269–282.
Sengor, A.M.C., Gorur, N., Saroglu, F., 1985. Strike-slip faulting and related basin formation in zones of tectonic escape: Turkey as a case study. In: Biddle, K., Christie-Blick, N. (Eds.), Strike-slip Faulting and Basin Formation. Society of Economic Paleontologists and Mineralogists, Special Publication 37, Tulsa, OK.
Tan, O., Taymaz, T., January 27 2003. M_w = 6.0, Pulumur earthquake focal mechanism solution. In: Earthquake Symposium, Kocaeli, Turkey, p. 11 (in Turkish).
Tuysuz, O., Erturac, M.K., 2005 March 12 and 14. Karliova Earthquakes and Thoughts. ITU Eurasia Earth Science Institute, Istanbul, Turkey (in Turkish).
Wessel, P., Smith, W.H.F., 2001. The Generic Mapping Tools (GMT) Version 3.4 Technical Reference & Cookbook. SOEST/NOAA.